

Quantum Chromodynamics, Antiferromagnets and XY Models from a Unified Point of View

Christoph P. Hofmann^a

^a Facultad de Ciencias, Universidad de Colima
Bernal Díaz del Castillo 340, Colima C.P. 28045, Mexico

October 25, 2016

Abstract

Antiferromagnets and quantum XY magnets in three space dimensions are described by an effective Lagrangian that exhibits the same structure as the effective Lagrangian of quantum chromodynamics with two light flavors. These systems all share a spontaneously broken internal symmetry $O(N) \rightarrow O(N-1)$. Although the respective scales differ by many orders of magnitude, the general structure of the low-temperature expansion of the partition function is the same. In the nonabelian case, logarithmic terms of the form $T^8 \ln T$ emerge at three-loop order, while for $N=2$ the series only involves powers of T^2 . The manifestation of the Goldstone boson interaction in the pressure, order parameter, and susceptibility is explored in presence of an external field.

1 Motivation

The systematic effective Lagrangian method is well-established in particle physics. The prime example is chiral perturbation theory – the low-energy effective field theory of quantum chromodynamics (QCD). The same techniques can be applied to condensed matter systems whenever their low-energy physics is dominated by Goldstone bosons. In the present study, we consider $d=3+1$ dimensional systems characterized by a spontaneously broken internal symmetry $O(N) \rightarrow O(N-1)$. This includes collective quantum magnetism: antiferromagnets ($N=3$) and quantum XY magnets ($N=2$) – but it also covers particle physics, namely two-flavor QCD ($N=4$). We present the

evaluation of the partition function up to three-loop order and discuss the impact of the Goldstone boson interaction at low temperatures and in presence of an explicit symmetry breaking parameter (magnetic field, staggered field, nonzero quark mass).

Whereas the microscopic Hamiltonians of the quantum XY model and the Heisenberg antiferromagnet are invariant under $O(2)$ and $O(3)$, respectively, their ground states with antialigned spins, are not – the staggered magnetization vector, i.e. the order parameter, is different from zero. The spontaneously broken symmetry is only approximate because the staggered field explicitly breaks $O(2)$ and $O(3)$. Accordingly, the magnons or spin-waves that represent the Goldstone bosons, develop an energy gap. The case $O(4) \rightarrow O(3)$ is locally isomorphic to $SU(2) \times SU(2) \rightarrow SU(2)$ and hence describes quantum chromodynamics with a massless up- and down-quark exhibiting a spontaneously broken chiral symmetry. In nature, chiral symmetry is only approximate: the quark masses are nonzero and therefore the Goldstone bosons – the pions – have a small mass.

Appreciating the universal nature of the effective field theory method, we identify differences and analogies between systems as disparate as quantum magnets and quantum chromodynamics. The structure of the low-temperature expansion is an immediate consequence of the spontaneously broken symmetry. Also the question whether or not logarithmic terms of the form $T^n \ln T$ appear in the low-temperature series, can be answered from a universal point of view. The specific nature of the system only reflects itself in the actual numerical values of a few low-energy effective constants.

In the free energy density, the first correction to the leading free Bose gas term ($\propto T^4$) is of order T^6 . As we demonstrate, a logarithmic term $T^8 \ln T$ emerges at next-to-next-to-leading order (NNLO), provided that we are dealing with a nonabelian symmetry ($N \geq 3$). Likewise, in the order parameter and the susceptibility, logarithmic contributions show up. On the other hand, in the abelian case, the temperature series are characterized by simple powers of T^2 .

The Goldstone boson interaction in the pressure – depending on the strength of the external field and the specific N – may be repulsive, attractive, or zero at low temperatures. Regarding the order parameter and the susceptibility, counterintuitive effects may occur: the T -dependent interaction contribution in the order parameter (susceptibility) may become positive (negative). It should be noted that in QCD where the quark masses ("external field") are fixed at their nonzero values, no such counterintuitive effects occur at low temperatures in the physical region where the pion mass is $M_\pi \approx 139.6 \text{ MeV}$: going from $T=0$ to finite temperature, the T -dependent interaction contribution in the quark condensate (susceptibility) is negative (positive).

Before the systematic effective field theory analysis of the $d=3+1$ quantum XY model [1], the properties of this system at low temperatures where the spin waves dominate the physics, were only known to one-loop accuracy (see, e.g., Refs. [2–11]).

In the case of the Heisenberg antiferromagnet, the low-temperature series for the staggered magnetization has been reported in the pioneering article by Oguchi [12], but he apparently missed – much like subsequent investigators [13–23] – logarithmic terms $T^n \ln T$ in the low-temperature series. This demonstrates the power of the effective Lagrangian method in the condensed matter domain: in the present applications it proves to be superior to standard methods like spin-wave theory. On the other hand, the properties of quantum chromodynamics at finite temperatures have been the subject of many publications (see, e.g., Refs. [24–36]). Still, some additional material is presented here that is new to the best of our knowledge.

The article is organized as follows. The microscopic – or underlying – theories, as well as the corresponding effective Lagrangians, are briefly discussed in Sec. 2. The results for general N are presented in Sec. 3, where we focus on the structure of the low-temperature expansion for the free energy density. In Sec. 4, the low-temperature series for the pressure, order parameter and susceptibility are considered. The impact of the Goldstone-boson interaction in these observables is illustrated in various figures. In Sec. 5 we finally present our conclusions. Technical details of the calculation are contained in an appendix.

2 Underlying Versus Effective Description

Chiral perturbation theory has been transferred to condensed matter systems in Ref. [37], and the formalism has been generalized in Ref. [38]. Here we focus on finite-temperature effective field theory – outlines going beyond the brief sketch presented in this section, can be found in Ref. [1] and the references provided there.

The microscopic Hamiltonian for the antiferromagnetic quantum XY model in $d=3+1$ is given by

$$\mathcal{H} = -J \sum_{\langle xy \rangle} (S_x^1 S_y^1 + S_x^2 S_y^2) - \vec{H}_s \cdot \sum_x (-1)^{\frac{x_1+x_2+x_3}{a}} \vec{S}_x, \quad J < 0. \quad (2.1)$$

The summation $\langle xy \rangle$ extends over all pairs of nearest neighbors on a simple cubic lattice, separated by the distance \hat{a} . The quantity J is the exchange integral, and $\vec{H}_s = (H_s, 0)$ is the staggered field pointing into the 1-direction in the XY plane. The model can be extended by including the third spin component,

$$\begin{aligned} \mathcal{H} &= -J \sum_{\langle xy \rangle} (S_x^1 S_y^1 + S_x^2 S_y^2 + S_x^3 S_y^3) - \vec{H}_s \cdot \sum_x (-1)^{\frac{x_1+x_2+x_3}{a}} \vec{S}_x, \quad J < 0, \\ \vec{H}_s &= (H_s, 0, 0), \end{aligned} \quad (2.2)$$

which defines the Heisenberg antiferromagnet in a staggered field. It should be noted that on a bipartite lattice – and only for the abelian case $N=2$ – there is a one-to-one

correspondence between the XY quantum antiferromagnet in a staggered field and the ferromagnetic ($J > 0$) quantum XY model in a magnetic field.

At zero temperature and infinite volume, the staggered magnetization Σ_s and the spontaneous magnetization Σ are different from zero,

$$\begin{aligned}\Sigma_s &= \langle 0 | \sum_x (-1)^{(x_1+x_2+x_3)/\hat{a}} S_x^1 | 0 \rangle / V, & (N = 2, 3) \\ \Sigma &= \langle 0 | \sum_x S_x^1 | 0 \rangle / V, & (N = 2)\end{aligned}\tag{2.3}$$

indicating that the $O(N)$ symmetry is spontaneously broken. As a consequence, $N-1$ Goldstone bosons emerge – these are the well-known spin waves or magnons.

We now leave quantum magnetism and consider the strong interaction. The QCD Lagrangian with two light quarks is given by

$$\mathcal{L}_{QCD} = -\frac{1}{2g^2} \text{tr}_c G_{\mu\nu} G^{\mu\nu} + \bar{q} i \gamma^\mu D_\mu q - \bar{q} m q, \quad (q = u, d), \tag{2.4}$$

where all quantities have the usual meaning (see e.g. Ref. [40]).¹ The quark condensate

$$\langle 0 | \bar{u} u | 0 \rangle = \langle 0 | \bar{d} d | 0 \rangle \tag{2.5}$$

represents the order parameter, its nonzero value signaling that the chiral symmetry $SU(2) \times SU(2) \approx O(4)$ is spontaneously broken. The three pions are the Goldstone bosons, originating from the spontaneously broken chiral symmetry.

The low-energy physics of all three systems – XY models, Heisenberg antiferromagnets and quantum chromodynamics – is thus dominated by the corresponding Goldstone bosons, such that the effective Lagrangian method (“chiral perturbation theory” in the context of QCD) can be applied. In the following we assume that we are dealing with a spontaneously broken symmetry $O(N) \rightarrow O(N-1)$, keeping in mind that the cases $N = \{2, 3, 4\}$ refer to the physical realizations of interest.

The Goldstone boson physics is universal: the specific terms in the effective Lagrangian are a consequence of the symmetries of the underlying (microscopic) theory. A particular physical realization then corresponds to a specific numerical set of low-energy effective constants. Whereas the respective scales involved may differ by many orders of magnitude, the structure of the low-energy (low-temperature) expansion is universal.

The leading term in the effective Lagrangian that describes the symmetry breaking pattern $O(N) \rightarrow O(N-1)$, is of order p^2 as it contains two derivatives,

$$\mathcal{L}_{eff}^2 = \frac{1}{2} F^2 \partial_\mu U^i \partial^\mu U^i + \Sigma_s H_s^i U^i. \tag{2.6}$$

¹In the following we refer to the *isospin limit* where the two light quark masses are identical: $m_u = m_d$.

The $N-1$ Goldstone bosons that dominate the low-energy physics are contained in the unit vector U^i

$$U^i = (U^0, U^a), \quad U^0 = \sqrt{1 - U^a U^a}, \quad a = 1, 2, \dots, N-1. \quad (2.7)$$

Note that we are actually dealing with (pseudo-)Goldstone bosons: in presence of an external field H_s , the Goldstone bosons become massive

$$\omega = \sqrt{v^2 \vec{k}^2 + v^4 M^2}. \quad (2.8)$$

In the context of magnetic systems, v is the spin-wave velocity that we set to one. The relation between the Goldstone boson mass and the external field is given by

$$M^2 = \frac{\Sigma_s H_s}{F^2}. \quad (2.9)$$

At leading order we have two low-energy effective constants: F ("pion decay constant" in QCD) and Σ_s (order parameter at zero temperature and infinite volume). The next-to-leading order effective Lagrangian is of order p^4 ,

$$\begin{aligned} \mathcal{L}_{eff}^4 = & e_1 (\partial_\mu U^i \partial^\mu U^i)^2 + e_2 (\partial_\mu U^i \partial^\nu U^i)^2 + k_1 \frac{\Sigma_s}{F^2} (H_s^i U^i) (\partial_\mu U^k \partial^\mu U^k) \\ & + k_2 \frac{\Sigma_s^2}{F^4} (H_s^i U^i)^2 + k_3 \frac{\Sigma_s^2}{F^4} H_s^i H_s^i, \end{aligned} \quad (2.10)$$

and contains terms with up to four derivatives and up to two powers of the external field H_s that counts as order p^2 . The interpretation of the external field depends on context: magnetic field ($N=2$), staggered field ($N=2, 3$), nonzero quark mass ($N=4$). Note that \mathcal{L}_{eff}^4 involves five next-to-leading order (NLO) low-energy effective constants. In QCD, their numerical values are known – in connection with magnetic systems we have to estimate their size (see below).

While the QCD Lagrangian and the corresponding effective Lagrangian are Lorentz-invariant by construction, it is still legitimate to maintain a (pseudo-)Lorentz-invariant framework in connection with quantum magnetism on the effective level. First, the leading-order effective Lagrangian is strictly Lorentz-invariant (where $c = v \equiv 1$ is the spin-wave velocity): this is an accidental symmetry. Anisotropies start manifesting themselves at order p^4 : indeed, in \mathcal{L}_{eff}^4 one should take into account all terms that are allowed by, e.g., the cubic lattice geometry. However, the interaction part of the low-temperature expansion of the partition function is only affected at next-to-next-to leading order by these additional terms (see below), such that our conclusions are not altered. This is why it is justified to write \mathcal{L}_{eff}^4 in a (pseudo-)Lorentz-invariant form.

3 Results for the General Case $O(N) \rightarrow O(N-1)$

While the $d=3+1$ quantum XY model ($N=2$) has been discussed in Ref. [1], in the present study we focus on the nonabelian case $N \geq 3$ that includes antiferromagnets

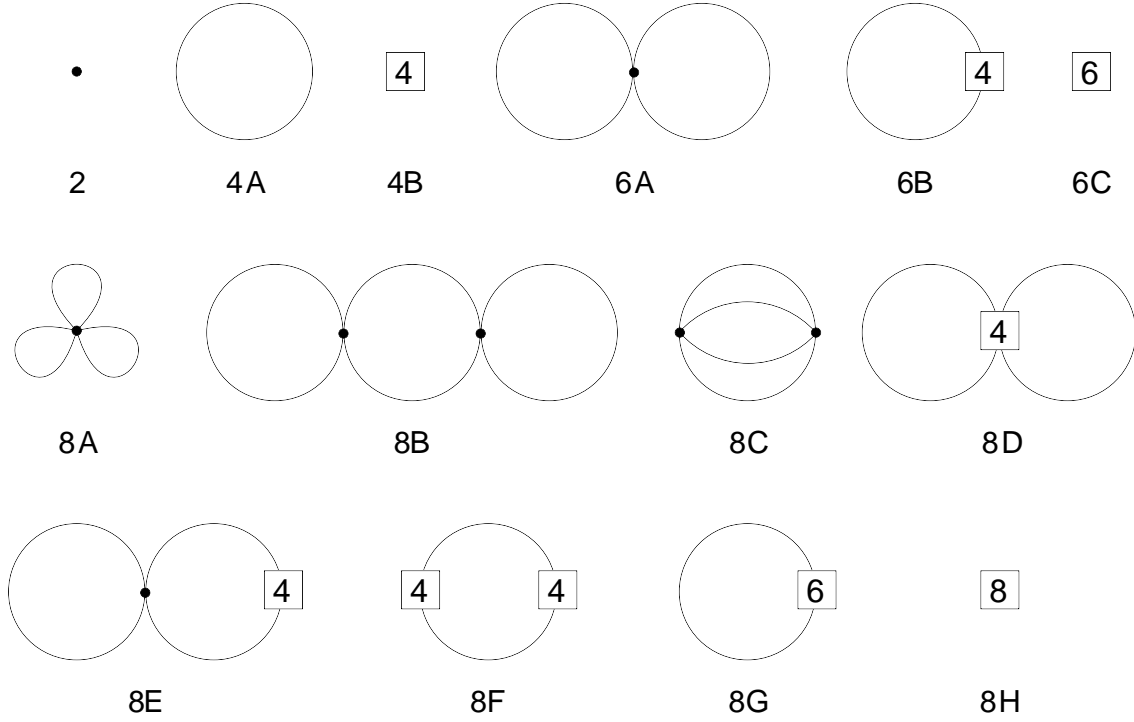


Figure 1: Feynman diagrams: Low-temperature expansion of the partition function up to three-loop order T^8 for $d=3+1$ dimensional systems with a spontaneously broken symmetry $O(N) \rightarrow O(N-1)$. Filled circles correspond to \mathcal{L}_{eff}^2 – vertices related to the higher-order pieces $\mathcal{L}_{eff}^4, \mathcal{L}_{eff}^6, \mathcal{L}_{eff}^8$ of the effective Lagrangian are denoted by the numbers 4, 6, 8. Each loop is suppressed by T^2 .

and quantum chromodynamics. The main observable of interest is the free energy density, from which the pressure, order parameter, and susceptibility can be derived. Details of the three-loop evaluation of the partition function can be found in the appendices of Refs. [1, 39]. In addition, pedagogic outlines on the effective Lagrangian method are provided by Refs. [40–42].

The Feynman diagrams needed up to three-loop order p^8 , are depicted in Fig. 1. Their evaluation leads to the following expression for the free energy density at low temperatures, valid for (pseudo-)Lorentz-invariant systems with a spontaneously broken internal symmetry $O(N) \rightarrow O(N-1)$:

$$z = z_0 - \frac{1}{2}(N-1)g_0 - 4\pi a(g_1)^2 - \pi g \left[b - \frac{j}{\pi^3 F^4} \right] + \mathcal{O}(p^{10}). \quad (3.1)$$

The individual quantities have the following meaning:² free energy density at $T=0$ (z_0 , Eq. (A.28)), kinematical functions (g_0, g_1, g , Eqs. (A.25) and (A.41)). On the other hand, for the parameters a, b , and the three-loop function j , the explicit expressions are provided below, as they all depend on N which leads to some subtle effects.

²In parenthesis we indicate where in appendix A of Ref. [1] the respective definitions can be found.

The functions g_0, g_1, g and j depend on the dimensionless ratio σ (or τ),

$$\sigma = \frac{M_\pi}{2\pi T}, \quad \tau = \frac{T}{M_\pi}, \quad (3.2)$$

where M_π is the Goldstone boson mass,

$$M_\pi^2 = \frac{\Sigma_s H_s}{F^2} + \left[2(k_2 - k_1) + (N - 3)\lambda \right] \frac{(\Sigma_s H_s)^2}{F^6} + c \frac{(\Sigma_s H_s)^3}{F^{10}} + \mathcal{O}(H_s^4). \quad (3.3)$$

The parameters a and b in Eq. (3.1) involve NLO effective constants and read

$$\begin{aligned} a &= -\frac{(N-1)(N-3)}{32\pi} \frac{\Sigma_s H_s}{F^4} + \frac{N-1}{4\pi} \frac{(\Sigma_s H_s)^2}{F^8} \left\{ \left[(N+1)(e_1 + e_2) + k_2 - k_1 \right] \right. \\ &\quad \left. - \frac{(N-1)^2}{2} \lambda - \frac{3N^2 + 32N - 67}{768\pi^2} \right\}, \\ b &= \frac{N-1}{\pi F^4} \left\{ \left[2e_1 + Ne_2 \right] - \frac{5(N-2)}{3} \lambda - \frac{N-2}{16\pi^2} \right\}. \end{aligned} \quad (3.4)$$

Note that λ ,

$$\begin{aligned} \lambda &= \frac{1}{2} (4\pi)^{-d/2} \Gamma(1 - \tfrac{1}{2}d) M^{d-4} \\ &= \frac{M^{d-4}}{16\pi^2} \left[\frac{1}{d-4} - \frac{1}{2} \{ \ln 4\pi + \Gamma'(1) + 1 \} + \mathcal{O}(d-4) \right], \end{aligned} \quad (3.5)$$

is singular in the limit $d \rightarrow 4$. The point is that this infinity can be absorbed by the NLO effective constants that show up in M_π^2, a, b . Whether e_1, e_2, k_1, k_2 get renormalized logarithmically or do not require renormalization, depends on N . Inspecting the N -dependence of b and M_π^2 , one notices the following subtleties. The parameter λ does not appear in b if $N=2$ – therefore, in this case, the combination $e_1 + e_2$ of NLO effective constants is finite and does not require logarithmic renormalization. Similarly, for $N=3$, the second term in the renormalized mass M_π^2 is free of λ – here the combination $k_2 - k_1$ is finite and no logarithmic renormalization is needed. In all other cases (including a), the NLO effective constants are renormalized logarithmically. The explicit renormalized expressions for M_π^2, a and b , along with more details on the renormalization procedure, can be found in the appendix.

Finally, the quantity j in Eq. (3.1) is defined by

$$I = \frac{1}{\pi^2} g j, \quad (3.6)$$

where I contains the contributions from the three-loop graphs 8A-C and reads

$$\begin{aligned} I &= \frac{1}{48} (N-1)(N-3) M_\pi^4 \bar{J}_1 - \frac{1}{4} (N-1)(N-2) \bar{J}_2 \\ &\quad - \frac{1}{16} (N-1)(N-3)^2 M_\pi^4 (g_1)^2 g_2 + \frac{1}{48} (N-1)(N-3)(3N-7) M_\pi^2 (g_1)^3. \end{aligned} \quad (3.7)$$

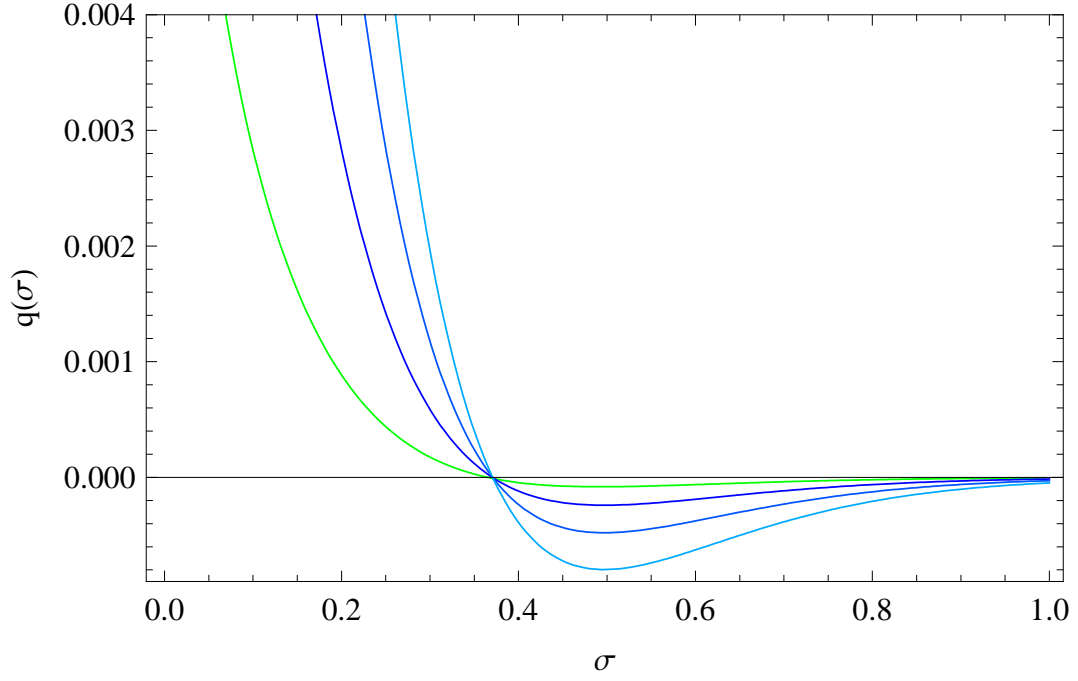


Figure 2: [Color online] The three-loop function $q(\sigma)$ in terms of the parameter $\sigma = M_\pi/2\pi T$ for $N = \{3, 4, 5, 6\}$ from top to bottom in the figure (vertical cut at $\sigma = 0.5$).

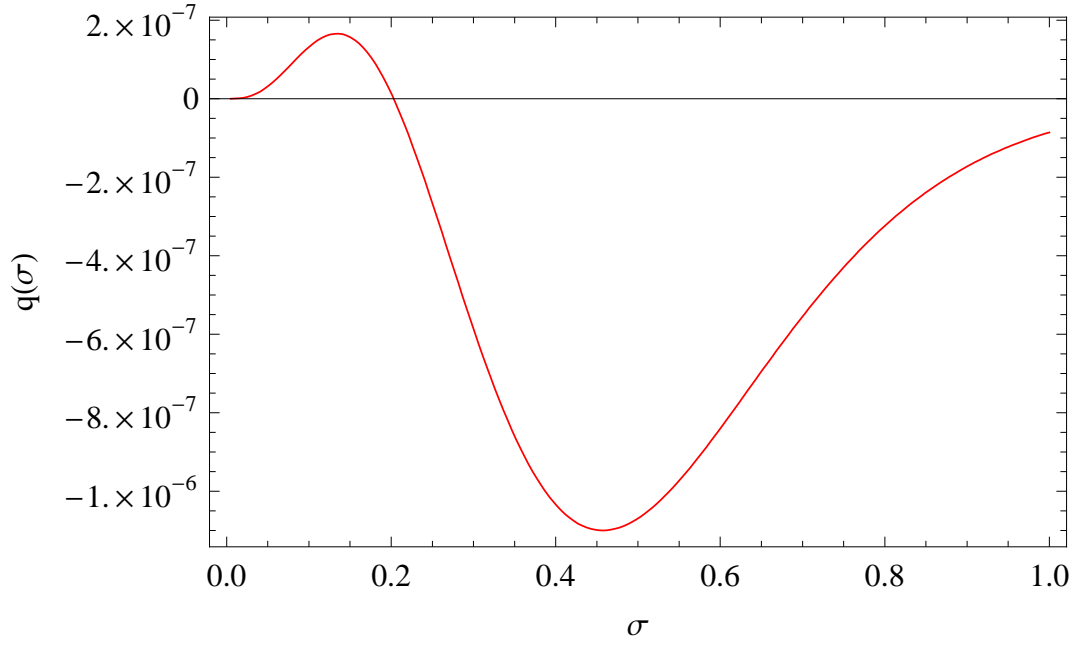


Figure 3: [Color online] The three-loop function $q(\sigma)$ in terms of the parameter $\sigma = M_\pi/2\pi T$ for $N=2$.

The numerical evaluation of the renormalized three-loop integrals \bar{J}_1 and \bar{J}_2 has been described in Ref. [24], and a graph for the function j has been provided there for the specific case $N=4$. However, here we are interested in arbitrary $N \geq 2$ – accordingly, we have to evaluate \bar{J}_1 and \bar{J}_2 individually. This quite involved task has been performed in Ref. [1] for \bar{J}_1 . The numerical evaluation of \bar{J}_2 , along the lines described in section 3 and the appendix of Ref. [24], has been performed in the present study. In Fig. 2 we show the resulting graphs for the function $q(\sigma)$,

$$\begin{aligned} T^8 q(\sigma) &= \frac{1}{48}(N-1)(N-3)M_\pi^4 \bar{J}_1 - \frac{1}{4}(N-1)(N-2)\bar{J}_2 \\ &= \frac{1}{48}(N-1)(N-3)q_1(\sigma) T^8 - \frac{1}{4}(N-1)(N-2)q_2(\sigma) T^8, \end{aligned} \quad (3.8)$$

for the cases $N = \{3, 4, 5, 6\}$. For completeness, in Fig. 3, we depict $q(\sigma)$ for the abelian case $N=2$. We also have checked consistency with Ref. [24]: setting $N=4$ indeed leads to the curve for j displayed in figure 2 of that reference.³

4 Low-Temperature Series

The effective field theory representations that we consider in this section are valid at low temperatures and weak external fields. This means that both T and M (i.e., H_s) have to be small with respect to a typical scale Λ that defines the microscopic system under consideration. Concretely one may choose

$$T, M, H_s \lesssim 0.2 \Lambda. \quad (4.1)$$

In quantum chromodynamics, Λ is the renormalization group invariant scale $\Lambda_{QCD} \approx 1\text{GeV}$. In Heisenberg or XY magnets, the underlying scale can be identified with the exchange integral $J \approx 1\text{meV}$. Regarding QCD, the leading-order effective constant F and the underlying scale Λ are connected by [43]

$$\Lambda = 4\pi F. \quad (4.2)$$

In the subsequent discussion, we assume that this relation is also valid for $N \neq 4$. Note that Eq. (4.2) refers to $d=3+1$ – a generalization to arbitrary dimensions has been given in [44].

4.1 Pressure

Let us now discuss the low-temperature representation for the pressure,

$$P = z_0 - z. \quad (4.3)$$

³Note that the function j contains all contributions of I (see Eqs. (3.6) and (3.7)), whereas the function q , Eq. (3.8), only involves the first two terms of I .

In order to display the explicit structure of T -powers, we introduce dimensionless functions $h_i(\sigma)$ and $h(\sigma)$ as follows:

$$\begin{aligned} g_0(\sigma) &= T^4 h_0(\sigma), & g_1(\sigma) &= T^2 h_1(\sigma), & g(\sigma) &= T^8 h(\sigma), \\ g_2(\sigma) &= h_2(\sigma), & g_3(\sigma) &= \frac{h_3(\sigma)}{T^2}, & \sigma &= \frac{M_\pi}{2\pi T}. \end{aligned} \quad (4.4)$$

For $N=2$ we then obtain

$$\begin{aligned} P(T, H_s) &= p_1(\tau) T^4 + p_2(\tau) T^6 + p_3(\tau) T^8 + \mathcal{O}(T^{10}), & (N=2) \\ p_1(\tau) &= \frac{1}{2} h_0(\sigma), \\ p_2(\tau) &= \frac{1}{8F^2 t^2} h_1(\sigma)^2, \\ p_3(\tau) &= \frac{3(e_1 + e_2) + \frac{1}{2}\bar{k} - \frac{3}{256\pi^2}}{F^4 \tau^4} h_1(\sigma)^2 + \frac{2(e_1 + e_2)}{F^4} h(\sigma) \\ &\quad - \frac{1}{\pi^2 F^4} j(\sigma) h(\sigma), \end{aligned} \quad (4.5)$$

where the renormalized coupling constant \bar{k} is defined in appendix A of Ref. [1].

In the nonabelian case ($N \geq 3$) we have

$$\begin{aligned} P(T, H_s) &= \tilde{p}_1(\tau) T^4 + \tilde{p}_2(\tau) T^6 + \tilde{p}_{3a}(\tau) T^8 + \tilde{p}_{3b} T^8 \ln\left(\frac{\Lambda_P}{T}\right) + \mathcal{O}(T^{10} \ln T), \\ \tilde{p}_1(\tau) &= \frac{1}{2}(N-1)h_0(\sigma), \\ \tilde{p}_2(\tau) &= -\frac{(N-1)(N-3)}{8F^2 t^2} h_1(\sigma)^2, \\ \tilde{p}_{3a}(\tau) &= \frac{(N-1)}{32\pi^2 F^4 \tau^4} \left\{ (N+1)(\tilde{\gamma}_1 \bar{e}_1 + \tilde{\gamma}_2 \bar{e}_2) + \tilde{\gamma}_4 \bar{k}_2 - \tilde{\gamma}_3 \bar{k}_1 - \frac{3N^2 + 32N - 67}{24} \right\} \\ &\quad \times h_1(\sigma)^2 + \frac{N-1}{32\pi^2 F^4} \left\{ 2\tilde{\gamma}_1 \bar{e}_1 + N\tilde{\gamma}_2 \bar{e}_2 - 2(N-2) \right\} \tilde{h}(\sigma) \\ &\quad - \frac{1}{F^4} \left\{ \frac{\pi^2}{675} \tilde{j}(\sigma) + \frac{j(\sigma)\tilde{h}(\sigma)}{\pi^2} \right\}, \\ \tilde{p}_{3b}(\tau) &= \frac{(N-1)(N-2)\pi^2}{6480F^4}. \end{aligned} \quad (4.6)$$

The renormalized NLO effective coupling constants $\bar{e}_1, \bar{e}_2, \bar{k}_1, \bar{k}_2$, the quantities $\tilde{\gamma}_1, \tilde{\gamma}_2, \tilde{\gamma}_3, \tilde{\gamma}_4$, the functions $\tilde{h}(\tau)$ and $\tilde{j}(\tau)$, as well as the scale Λ_P , are defined in the appendix.⁴ We have checked that for $N=4$ the coefficients $\tilde{p}_i(\tau)$ coincide with the known results for quantum chromodynamics at low temperatures, given explicitly in Ref. [24].

⁴Note that the two-loop contribution, both in the abelian $[p_2(\tau)]$ and the nonabelian $[\tilde{p}_2(\tau)]$ case, involves the ratio $t = T/M$, rather than $\tau = T/M_\pi$. The two masses are related by Eqs. (2.9) and (3.3).

The Goldstone-boson interaction comes into play beyond the free Bose gas term of order T^4 . We define three classes of systems, according to the sign of $p_2(\tau)$ and $\tilde{p}_2(\tau)$ that are associated with the dominant (two-loop) correction of order T^6 . In QCD, or for any other system with $N \geq 4$, the prefactor is negative and we are dealing with an attractive interaction among the Goldstone bosons. On the other hand, in the quantum XY model (or any other realization of $N=2$), the prefactor is positive, signaling a repulsion among the magnons. Finally, for the antiferromagnet ($N=3$) the two-loop term vanishes.

Interestingly, up to two-loop order, the low-temperature representation for the pressure exclusively involves powers of T^2 . However, at the three-loop level, logarithmic contributions of the form $T^8 \ln T$ show up in the *nonabelian* case. In fact, the three-loop function $q(\sigma)$, Eq. (3.8),

$$T^8 q(\sigma) = \frac{1}{48}(N-1)(N-3)q_1(\sigma)T^8 - \frac{1}{4}(N-1)(N-2)q_2(\sigma)T^8,$$

dictates whether or not such logarithms occur. The crucial piece is $q_2(\sigma)$, as it depends logarithmically on the parameter σ or – equivalently – on $\tau = 1/(2\pi\sigma)$. In the abelian case, only $q_1(\sigma)$ is relevant: this function does not depend logarithmically on σ and one concludes that the three-loop contribution in the pressure then only involves a simple power T^8 – no additional contribution $T^8 \ln T$ arises in the abelian case. The explicit steps that lead to the representations (4.5) and (4.6) for the pressure can be found in the appendix.

Remarkably, for $N \geq 3$, in the limit $H_s, M_\pi \rightarrow 0$ only the logarithmic contribution that involves the scale Λ_P survives – the other terms ($\propto T^8$ and $\propto T^6$) tend to zero. In the absence of an external field, the interaction contribution in the pressure is thus dominated by the logarithm $T^8 \ln T$.

It should be pointed out that the presence or absence of logarithmic terms in the low-temperature representations is not an artifact of our idealization concerning (pseudo-)Lorentz-invariance. The cateye graph 8C that defines the function $q_2(\sigma)$, exclusively involves the leading-order piece \mathcal{L}_{eff}^2 that is strictly (pseudo-)Lorentz-invariant. The anisotropies of, e.g., the simple cubic lattice start manifesting themselves at order \mathcal{L}_{eff}^4 and cannot affect the function $q(\sigma)$.

For the subsequent plots that illustrate the strength of the Goldstone-boson interaction, we need to know the numerical values of the renormalized NLO effective constants $\bar{e}_1, \bar{e}_2, \bar{k}_1$ and \bar{k}_2 . As described, e.g., in Ref. [45], these (dimensionless) constants are of order one (see also appendix C of Ref. [1]),⁵

$$\bar{e}_1, \bar{e}_2, \bar{k}_1, \bar{k}_2 \approx 1. \quad (4.7)$$

⁵It should be noted that we follow the standard convention of chiral perturbation theory, Eq. (A.3), where a factor of $1/32\pi^2$ is introduced in the relation between renormalized and unrenormalized NLO effective constants. In Ref. [1] we used a different convention (no factor of $1/32\pi^2$).

In quantum chromodynamics, the values of the NLO effective constants (both their magnitude and sign) are known quite accurately. Those relevant for our analysis are [46, 47]⁶

$$\bar{l}_1 = -0.36 \pm 0.6, \quad \bar{l}_2 = 4.31 \pm 0.1, \quad \bar{l}_3 = 3.0 \pm 0.8, \quad \bar{l}_4 = 4.39 \pm 0.2. \quad (4.8)$$

Notice that in our notation we have

$$\bar{e}_1 = \bar{l}_1, \quad \bar{e}_2 = \bar{l}_2, \quad \bar{k}_1 = \bar{l}_4, \quad \bar{k}_2 = \bar{l}_3 + \bar{l}_4. \quad (4.9)$$

Whereas the magnitude of $\bar{e}_1, \bar{e}_2, \bar{k}_1, \bar{k}_2$ can be estimated for arbitrary N , the sign of these effective constants – except for $N=4$ – remains open: it depends on the specific realization of a given N and must be determined for each system individually.

One way to obtain the accurate numerical values and the signs of these NLO effective constants in connection with quantum magnets, would be to compare the effective calculation with the analogous microscopic analysis – unfortunately, such two- or three-loop results in the parameter region of interest (low temperatures, weak external fields) appear to be unavailable. Another possibility to determine NLO effective constants would be through numerical simulation of the underlying model, or by experiment. However, Monte Carlo simulations in the relevant parameter region, or experimental results seem to be lacking. This then means that we have to rely our discussion on the above estimates (except for QCD).

Let us now investigate the nature of the Goldstone boson interaction in presence of an external field H_s . In order to measure strength and sign of the interaction in the pressure, in Fig. 4 we depict the quantity

$$\xi_P(T, H_s) = \frac{P_{int}^{[6]}(T, H_s) + P_{int}^{[8]}(T, H_s)}{P_{Bose}(T, H_s)} \quad (4.10)$$

for the temperature $T/F = 0.04$ and $N = \{2, 3, 4, 5, 6\}$. The dashed curves show the two-loop contribution ($P_{int}^{[6]}$), while the continuous curves refer to the sum of the two-loop and the three-loop correction ($P_{int}^{[6]} + P_{int}^{[8]}$). Since the signs of the effective constants $\bar{e}_1, \bar{e}_2, \bar{k}_1, \bar{k}_2$, in general, are unknown, we have scanned each of these couplings in the interval

$$\{\bar{e}_1, \bar{e}_2, \bar{k}_1, \bar{k}_2\} \subset [-5, 5], \quad (4.11)$$

in order to draw the three-loop correction. Note that these numbers correspond to the scale $\mu = \hat{M}_\pi$ – according to Eq. (A.10), the values of the effective constants $\bar{e}_1, \bar{e}_2, \bar{k}_1, \bar{k}_2$ depend on M_π , i.e., on the external field H_s . Of course, this dependence has been taken into account in the figures. On the other hand, the quantities $\tilde{\gamma}_1, \tilde{\gamma}_2, \tilde{\gamma}_3$ and $\tilde{\gamma}_4$ obey Eqs. (A.7) and (A.8).

In Fig. 4 and all subsequent figures, we depict the two extreme situations for $\xi_P(T, H_s)$: the maximal and the minimal three-loop corrections that we obtain from

⁶As we discuss in the appendix, the quantities $\bar{l}_1, \dots, \bar{l}_4$ have been evaluated at the scale $\mu = \hat{M}_\pi$.

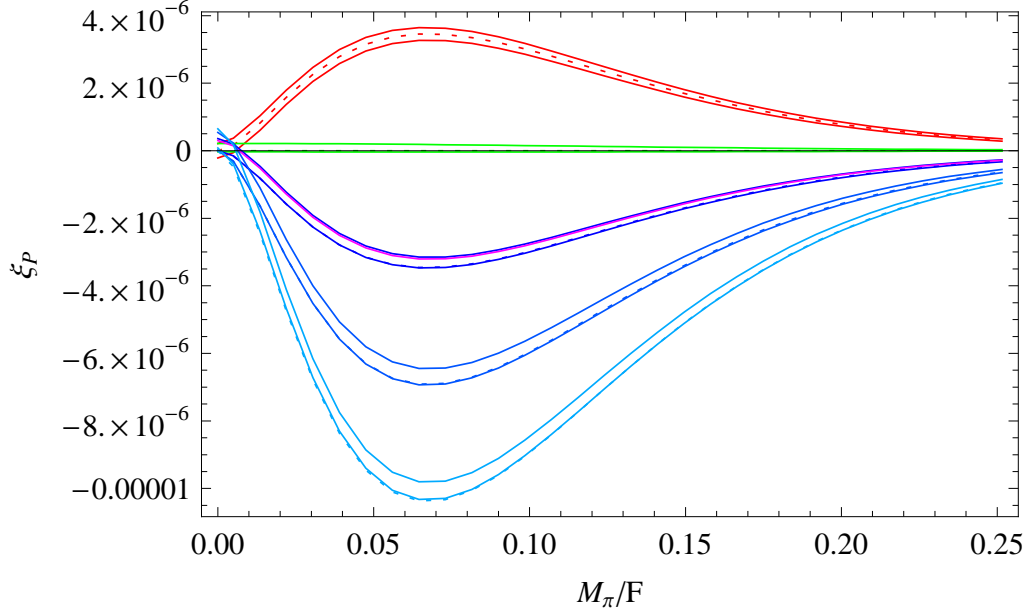


Figure 4: [Color online] Goldstone-boson interaction manifesting itself in the pressure of $d=(3+1)$ systems characterized by a spontaneously broken symmetry $O(N) \rightarrow O(N-1)$ for $N = \{2, 3, 4, 5, 6\}$ from top to bottom in the figure: two-loop contribution (dashed curves) and sum of two-loop contribution and three-loop correction (continuous curves). The temperature is $T/F = 0.04$.

these scans – this corresponds to an upper and lower bound for the three-loop contribution. In the case of QCD, where both sign and magnitude of the NLO low-energy constants and also the $\tilde{\gamma}_i$'s are known, we have highlighted the corresponding curve in magenta – it perfectly lies between the lower and upper estimates.

In QCD, the sign of the three-loop correction is positive and thus weakens the attractive two-loop contribution in the pressure. In particular, in the chiral limit ($M_\pi, H_s \rightarrow 0$) the interaction among the pions becomes repulsive.⁷ One notices that the three-loop correction for $N \neq 4$ in most scenarios also tends to be positive as in QCD. Still, depending on the actual values of the NLO LEC's and the $\tilde{\gamma}_i$'s, the three-loop correction in the pressure may be negative – in particular, the Goldstone-boson interaction in the pressure may be attractive if the external field is switched off. The three-loop corrections are quite small, but they grow when the temperature is raised, as we illustrate in Fig. 5.

In QCD at low temperatures, according to Fig. 4, the interaction among the pions is mainly attractive – only for very small ratios M_π/F it becomes repulsive. However, as shown in Fig. 6, the interaction eventually becomes repulsive in the whole parameter

⁷The *chiral limit* in QCD refers to the fictitious world where the quark masses, and therefore the pion masses, are set to zero. In analogy to QCD, here we also refer to $H_s \rightarrow 0$ as "chiral limit" when $N \neq 4$.

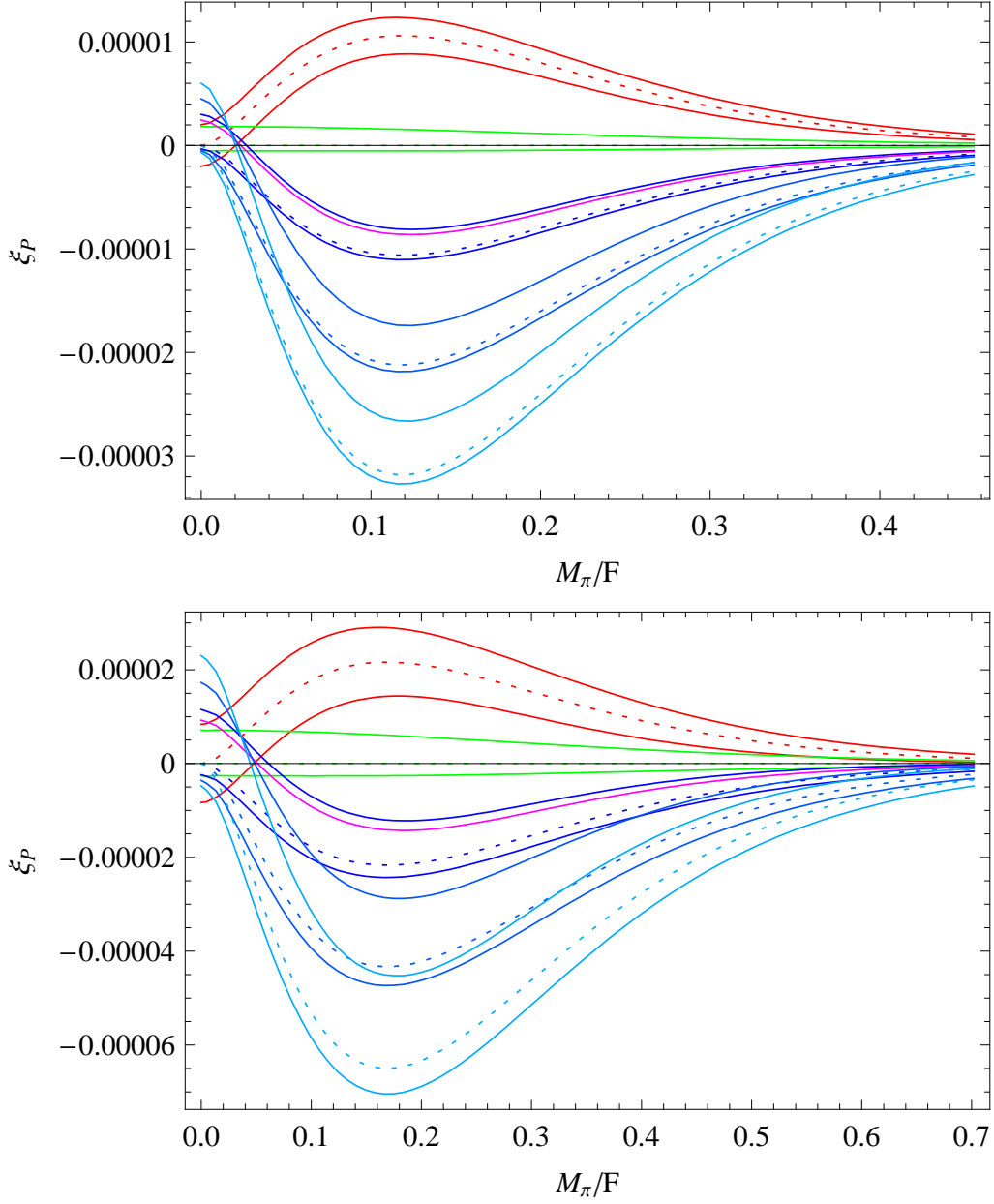


Figure 5: [Color online] Goldstone-boson interaction manifesting itself in the pressure of $d=(3+1)$ systems characterized by a spontaneously broken symmetry $O(N) \rightarrow O(N-1)$ for $N = \{2, 3, 4, 5, 6\}$ from top to bottom in the figure: two-loop contribution (dashed curves) and sum of two-loop contribution and three-loop correction (continuous curves). The temperatures are $T/F = 0.07, 0.10$ (top, bottom).

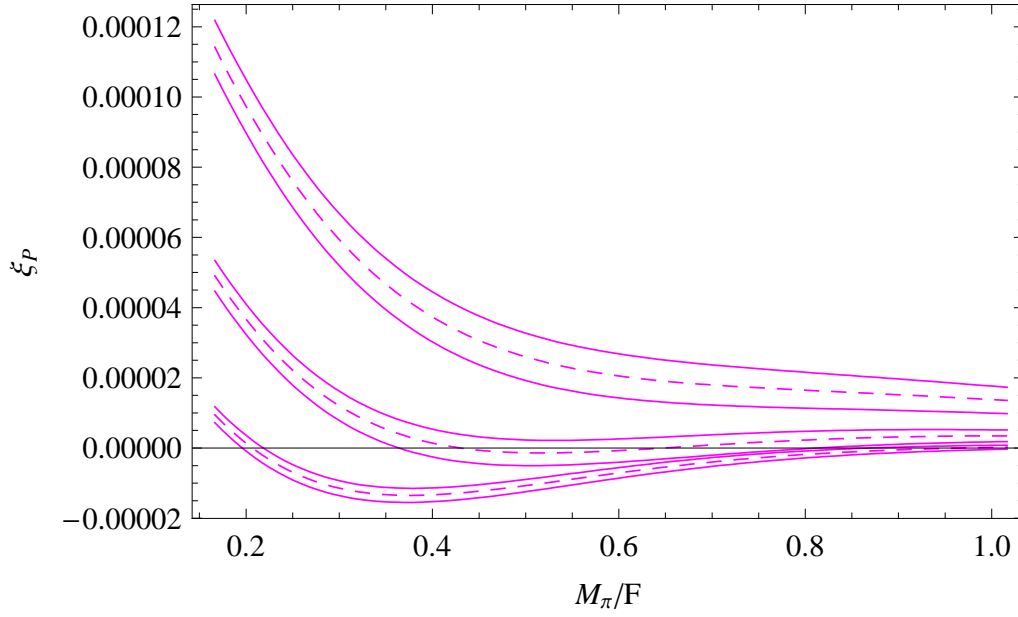


Figure 6: Quantum chromodynamics ($N=4$): Manifestation of the pion-pion interaction in the pressure. The curves refer to $T/F = \{0.17, 0.20, 0.23\}$ from bottom to top in the figure. The dashed curves correspond to the sum of the two- and three-loop correction. The error bars reflect the uncertainty in the values of the NLO effective constants $\bar{e}_1, \bar{e}_2, \bar{k}_1, \bar{k}_2$ – see Eqs. (4.8) and (4.9).

regime M_π/F , provided that the temperature exceeds $T/F \approx 0.20$: the (positive) three-loop corrections then become quite large. It should be pointed out that the interaction in the physical region – where the pion mass is fixed at $M_\pi \approx 139.6 \text{ MeV}$ – always is repulsive at low temperatures, and actually very weak: $\xi_P(T, M_\pi) \approx 10^{-6}$ for $T/F = 0.20$.

Unfortunately for systems with $N \neq 4$, as a consequence of the unknown signs of the NLO effective constants, the three-loop correction in the pressure may be positive or negative, as witnessed by the previous figures. Accordingly, the sum of the two-loop and three-loop contribution at more elevated temperatures may become repulsive in the entire parameter regime as in QCD. Again, to make concrete statements on the nature of the interaction, the values of $\bar{e}_1, \bar{e}_2, \bar{k}_1, \bar{k}_2$ and the $\tilde{\gamma}_i$'s not fixed by Eqs. (A.7) and (A.8), should be determined for each specific system – for instance by Monte Carlo simulations.

An important remark is finally in order here. Regarding the interaction one must distinguish between effects that already happen at zero temperature and those that occur at finite temperature. The fact that the physical Goldstone boson mass M_π and the bare Goldstone boson mass M are different, belongs to the first category: the corrections to the dominant contribution $M^2 = \Sigma_s H_s / F^2$ in M_π^2 , Eq. (3.3), result from the interaction at $T=0$. Note that it is M_π – and not M – that is relevant

in all our figures where we show the interaction contribution at *finite* temperature parametrized by M_π/F . The interpretation of the curves in our figures is thus the following: we begin at $T=0$ where the external field is switched on. Then we keep the field fixed, but go to finite temperature – the question then is whether switching on the temperature leads to an attraction or repulsion in the pressure.

4.2 Order Parameter

We now consider the order parameter, defined by

$$\Sigma_s(T, H_s) = -\frac{\partial z}{\partial H_s}. \quad (4.12)$$

Depending on context, this is the spontaneous magnetization ($N=2$), the staggered magnetization ($N = 2, 3$), or the quark condensate ($N=4$). With the representation of the free energy density, for $N=2$ we obtain

$$\begin{aligned} \Sigma_s(T, H_s) &= \Sigma_s(0, H_s) + \sigma_1(\tau)T^2 + \sigma_2(\tau)T^4 + \sigma_3(\tau)T^6 + \mathcal{O}(T^8), \\ \sigma_1(\tau) &= -\frac{\Sigma_s \hat{b}}{2F^2} h_1(\sigma), \\ \sigma_2(\tau) &= \frac{\Sigma_s}{8F^4} \left\{ h_1(\sigma)^2 - \frac{2\hat{b}}{t^2} h_1(\sigma) h_2(\sigma) \right\}, \\ \sigma_3(\tau) &= \frac{2\Sigma_s}{t^2 F^6} \left\{ 3(e_1 + e_2) + \frac{1}{2}\bar{k} - \frac{3}{256\pi^2} \right\} \left\{ h_1(\sigma)^2 - \frac{\hat{b}}{t^2} h_1(\sigma) h_2(\sigma) \right\} \\ &\quad - \frac{3\Sigma_s \hat{b}}{F^6} \left\{ 2(e_1 + e_2) - \frac{1}{\pi^2} j(\sigma) \right\} \left\{ h_0(\sigma) h_1(\sigma) + \frac{h_1(\sigma)^2 + h_0(\sigma) h_2(\sigma)}{\tau^2} \right\} \\ &\quad - \frac{3\Sigma_s \hat{b}}{8\pi^4 F^6 \sigma} \frac{\partial j(\sigma)}{\partial \sigma} \left\{ h_0(\sigma)^2 + \frac{h_0(\sigma) h_1(\sigma)}{\tau^2} \right\} - \frac{\Sigma_s}{64\pi^2 F^6 t^2} h_1(\sigma)^2. \end{aligned} \quad (4.13)$$

In the nonabelian case ($N \geq 3$) we have

$$\begin{aligned} \Sigma_s(T, H_s) &= \tilde{\Sigma}_s(0, H_s) + \tilde{\sigma}_1(\tau)T^2 + \tilde{\sigma}_2(\tau)T^4 + \tilde{\sigma}_{3a}(\tau)T^6 + \tilde{\sigma}_{3b}(\tau)T^6 \ln\left(\frac{\Lambda_\Sigma}{T}\right) \\ &\quad + \mathcal{O}(T^8 \ln T), \end{aligned} \quad (4.14)$$

with the coefficients

$$\begin{aligned} \tilde{\sigma}_1(\tau) &= -\frac{(N-1)\Sigma_s \hat{b}}{2F^2} h_1(\sigma), \\ \tilde{\sigma}_2(\tau) &= -\frac{(N-1)(N-3)\Sigma_s}{8F^4} \left\{ h_1(\sigma)^2 - \frac{2\hat{b}}{t^2} h_1(\sigma) h_2(\sigma) \right\}, \end{aligned} \quad (4.15)$$

$$\begin{aligned}
\tilde{\sigma}_{3a}(\tau) = & \frac{(N-1)\Sigma_s}{16\pi^2\tau^2 F^6} \left\{ (N+1)(\tilde{\gamma}_1\bar{e}_1 + \tilde{\gamma}_2\bar{e}_2) + \tilde{\gamma}_4\bar{k}_2 - \tilde{\gamma}_3\bar{k}_1 - \frac{3N^2 + 32N - 67}{24} \right\} \\
& \times \left\{ h_1(\sigma)^2 - \frac{\hat{b}}{\tau^2} h_1(\sigma)h_2(\sigma) \right\} - \frac{(N-1)\Sigma_s}{32\pi^2 F^6 \tau^2} \left\{ (N+1)(\tilde{\gamma}_1 + \tilde{\gamma}_2) + \tilde{\gamma}_4 - \tilde{\gamma}_3 \right\} \\
& \times h_1(\sigma)^2 - \frac{3(N-1)\Sigma_s\hat{b}}{32\pi^2 F^6} \left\{ 2\tilde{\gamma}_1\bar{e}_1 + N\tilde{\gamma}_2\bar{e}_2 - 2(N-2) \right\} \\
& \times \left\{ \frac{1}{12}\tilde{h}_0(\sigma) + \frac{\pi^2}{45}\tilde{h}_1(\sigma) + \tilde{h}_0(\sigma)\tilde{h}_1(\sigma) + \frac{h_1(\sigma)^2 + h_0(\sigma)h_2(\sigma)}{\tau^2} \right\} \\
& - \frac{(N-1)\Sigma_s\tau^2}{32\pi^2 F^6} \left\{ 2\tilde{\gamma}_1 + N\tilde{\gamma}_2 \right\} \left\{ \tilde{h}(\sigma) + \frac{\pi^4}{45}\sigma^2 \right\} \\
& + \frac{3\Sigma_s\hat{b}}{\pi^2 F^6} \left\{ \frac{1}{12}\tilde{h}_0(\sigma) + \frac{\pi^2}{45}\tilde{h}_1(\sigma) + \tilde{h}_0(\sigma)\tilde{h}_1(\sigma) + \frac{h_1(\sigma)^2 + h_0(\sigma)h_2(\sigma)}{\tau^2} \right\} j(\sigma) \\
& + \frac{\Sigma_s\hat{b}}{180F^6} \tilde{j}(\sigma) - \frac{\Sigma_s\hat{b}}{5400F^6\sigma} \left\{ \frac{\partial\tilde{j}(\sigma)}{\partial\sigma} - 8\pi^2 j_2\sigma \right\} - \frac{\Sigma_s\hat{b}}{8\pi^4 F^6\sigma} \frac{\partial\tilde{j}(\sigma)}{\partial\sigma} \tilde{h}(\sigma), \\
\tilde{\sigma}_{3b}(\tau) = & -\frac{(N-1)(N-2)\Sigma_s}{1728F^6}. \tag{4.16}
\end{aligned}$$

The parameter \hat{b} is

$$\hat{b}(H_s) = \frac{\partial M_\pi^2}{\partial M^2} = 1 + \frac{1}{16\pi^2} \left\{ \tilde{\gamma}_4(2\bar{k}_2 - 1) - \tilde{\gamma}_3(2\bar{k}_1 - 1) \right\} \frac{M^2}{F^2} + \mathcal{O}(H_s^2). \tag{4.17}$$

The Goldstone boson interaction in the order parameter manifests itself at order T^4 (two loops) and T^6 (three loops). Again, in the nonabelian case, logarithmic contributions of the form $T^6 \ln T$ occur at the three-loop level that involve the scale Λ_Σ that is defined in Eq. (A.20). Analogous to the pressure, the term $\propto T^6 \ln(\Lambda_\Sigma/T)$ survives in the limit $H_s, M_\pi \rightarrow 0$, whereas the other nonabelian three-loop contribution ($\propto T^6$) vanishes if the external field is switched off.

In order to measure strength and sign of the Goldstone boson interaction in the temperature-dependent part of order parameter, we consider the dimensionless quantity

$$\xi_\Sigma(T, H_s) = \frac{\Sigma_{int}^{[4]}(T, H_s) + \Sigma_{int}^{[6]}(T, H_s)}{|\Sigma_{Bose}(T, H_s)|}, \tag{4.18}$$

where the numerator contains the sum of the two- and three-loop contribution. For $N = \{2, 3, 4, 5, 6\}$, in Fig. 7, we depict the above ratio $\xi_\Sigma(T, H_s)$ for the temperatures $T/F = 0.04, 0.07, 0.10$, respectively. The dashed curves correspond to the two-loop contribution, while the continuous curves refer to the total correction (two-loop plus three-loop) that we obtained from the scans of NLO low-energy effective constants as described before. Note that in the case of the antiferromagnet, the spin-wave interaction only starts manifesting itself at three-loop order.

One notices that the three-loop corrections become quite large as the temperature rises. Depending on the specific realization of the model, $\xi_\Sigma(T, H_s)$ may be positive.

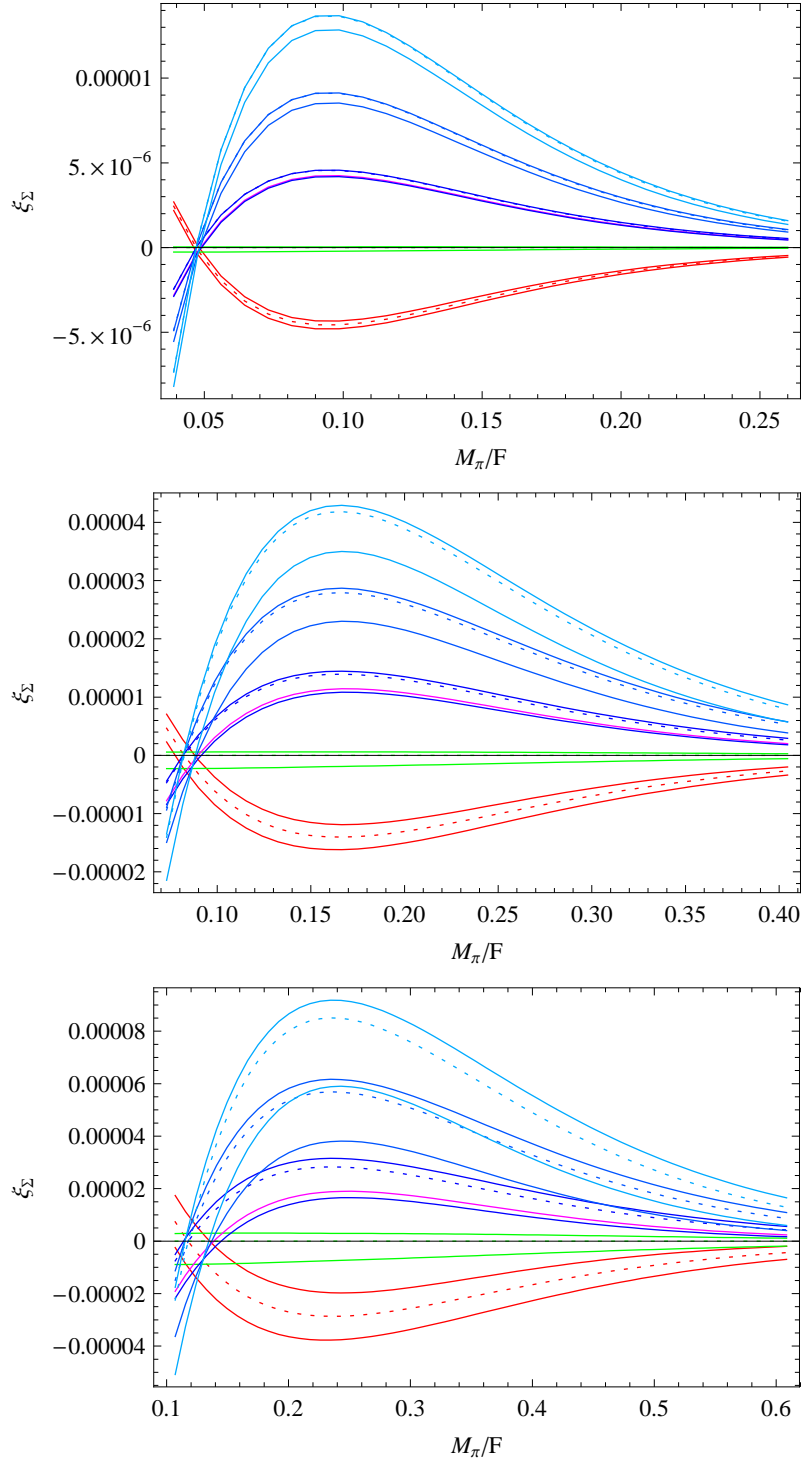


Figure 7: [Color online] Temperature-dependent Goldstone-boson interaction manifesting itself in the order parameter of $d=(3+1)$ systems characterized by a spontaneously broken symmetry $O(N) \rightarrow O(N-1)$ for $N = \{2, 3, 4, 5, 6\}$ from bottom to top in the figure (vertical cut at $M_\pi/F = 0.2$): two-loop contribution (dashed curves) and sum of two-loop contribution and three-loop correction (continuous curves). The temperatures are $T/F = 0.04, 0.07, 0.10$ (top to bottom).

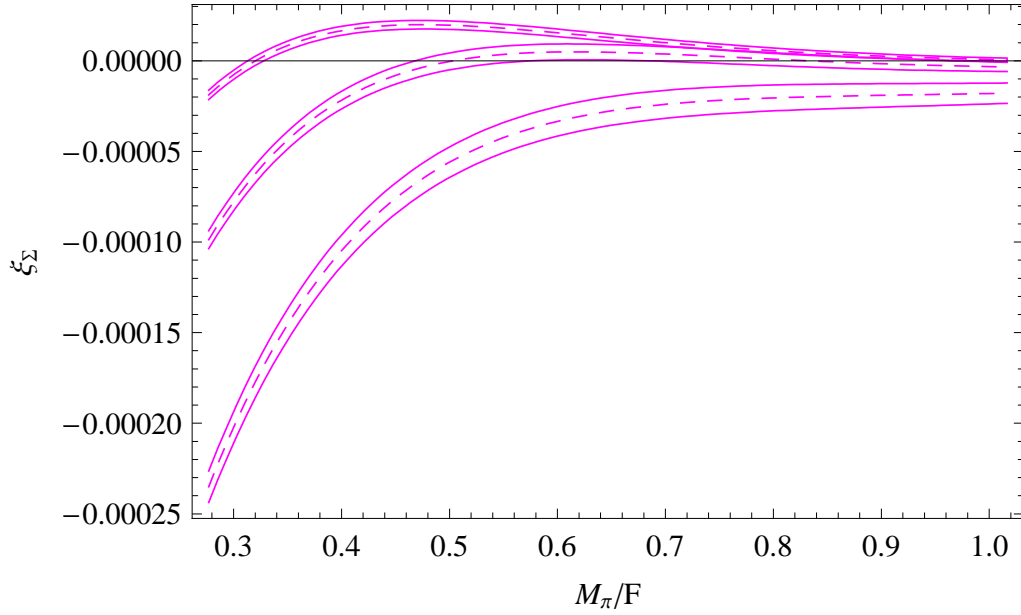


Figure 8: Quantum chromodynamics ($N=4$): Manifestation of the pion-pion interaction in the quark condensate. The curves refer to $T/F = \{0.17, 0.20, 0.23\}$ from top to bottom in the figure. The dashed curves correspond to the sum of the two- and three-loop correction. The error bars reflect the uncertainty in the values of the NLO effective constants $\bar{e}_1, \bar{e}_2, \bar{k}_1, \bar{k}_2$ – see Eqs. (4.8) and (4.9).

This is rather counterintuitive, because it means that the temperature-dependent interaction enhances the order parameter when we go from zero to finite temperature while keeping the external field fixed. This happens for the quantum XY model in weak external fields. For $N \geq 4$ and very low temperatures (see Fig. 7), it basically occurs in the entire region M_π/F depicted, except for weak fields where $\xi_\Sigma(T, H_s)$ drops to negative values.

In general, no definite conclusions regarding the sign of $\xi_\Sigma(T, H_s)$ are possible, because the signs of the NLO LEC's are unknown. The exception is QCD where the corresponding curves in magenta indicate that $\xi_\Sigma(T, H_s)$ is positive at low temperatures (except when approaching the chiral limit), but drops to negative values if the temperature is raised. Actually, if the temperature exceeds $T/F \approx 0.20$, $\xi_\Sigma(T, H_s)$ attains negative values for any of the ratios M_π/F that we have considered. This is illustrated in Fig. 8. In the physical region ($M_\pi \approx 139.6 \text{ MeV}$) the quantity $\xi_\Sigma(T, H_s)$ always is negative at low temperatures – but the effect of the interaction is very weak: $\xi_\Sigma(T, H_s) \approx -10^{-6}$ for $T/F = 0.20$. For QCD at the physical pion mass, there are thus no counterintuitive effects: if the temperature is raised while $M_\pi \approx 139.6 \text{ MeV}$ is kept fixed, the T -dependent interaction correction leads to a decrease of the quark condensate.

It should be pointed out that these two- and three-loop effects are very small. The

properties of the order parameter are in fact dominated by the one-loop contribution, which is negative in the entire parameter range for all N that we have considered. The respective term involves the quantity $-h_1$ that is negative (see Fig. 3 of Ref. [1]). As one expects, the order parameter decreases if the temperature is raised while keeping the external field fixed.

4.3 Susceptibility

Finally, we consider the susceptibility,

$$\chi(T, H_s) = \frac{\partial \Sigma_s(T, H_s)}{\partial H_s} = \frac{\Sigma_s}{F^2} \frac{\partial \Sigma_s(T, M)}{\partial M^2}, \quad (4.19)$$

that describes the response of the order parameter to the applied external field. Both in the abelian and the nonabelian case, we obtain

$$\begin{aligned} \chi(T, H_s) &= \chi(0, H_s) + \chi_1(\tau) + \chi_2(\tau)T^2 + \chi_3(\tau)T^4 + \mathcal{O}(T^6), \\ \chi_1(\tau) &= \frac{(N-1)\Sigma_s^2}{2F^4} \left\{ \hat{b} h_2(\sigma) - \frac{\hat{b}\tau}{4\pi} \frac{\partial \hat{b}}{\partial \sigma} h_1(\sigma) \right\}, \\ \chi_2(\tau) &= \frac{(N-1)(N-3)\Sigma_s^2}{8F^6} \left\{ \left[2(1 + \hat{b}) + \frac{\hat{b}\tau}{2\pi t^2} \frac{\partial \hat{b}}{\partial \sigma} \right] h_1(\sigma) h_2(\sigma) \right. \\ &\quad \left. - \frac{2\hat{b}}{t^2} \left(h_2(\sigma)^2 + h_1(\sigma) h_3(\sigma) \right) \right\}. \end{aligned} \quad (4.20)$$

The explicit expression for the three-loop contribution $\chi_3(\tau)$ turns out to be lengthy. As it can trivially be obtained from the representation of the order parameter, we do not list it here.

The temperature-dependent Goldstone boson interaction in the susceptibility shows up at order T^2 (two loops) and order T^4 (three loops). In contrast to the pressure and the order parameter, the susceptibility becomes singular in the chiral limit $M_\pi, H_s \rightarrow 0$. The dominant one-loop contribution diverges like

$$\lim_{H_s \rightarrow 0} \chi_1 \propto \frac{T}{\sqrt{H_s}} \propto \frac{T}{M}. \quad (4.21)$$

The two-loop and three-loop contributions also become singular as the external field tends to zero. Therefore the decomposition of the nonabelian three-loop contribution into two terms $\propto T^4$ and $\propto T^4 \ln(\Lambda_\chi/T)$ – in order to analyze the behavior of the system in the limit $M_\pi, H_s \rightarrow 0$ – is purely "academic". Unlike for the pressure and the order parameter, in the present case of the susceptibility, the three-loop terms diverge in the chiral limit and it makes no sense to introduce a scale Λ_χ . Remember that, concerning the pressure and the order parameter, the respective terms involving the

scales Λ_P and Λ_Σ remain finite in the chiral limit, while the other (non-logarithmic) contributions tend to zero.

The singular behavior of the one-loop contribution in the susceptibility has been reported for the $d=3+1$ quantum XY model in Ref. [5]. In quantum chromodynamics the divergence of the so-called disconnected chiral susceptibility has been reported first in Ref. [25], where two-loop corrections have been provided as well. We have to point out, however, that the analysis up to three-loop order presented here, appears to be new for any $N = \{2, 3, 4\}$, to the best of our knowledge.

In the context of quantum spin models ($N = 2, 3$), the external field corresponds to the staggered field $\vec{H}_s = (H_s, 0, 0)$, and the order parameter is identified with the staggered magnetization. Since \vec{H}_s tends to reinforce the antiparallel arrangement of the spins, one expects the order parameter to increase when the staggered field gets stronger – the staggered susceptibility $\chi(T, H_s)$ is therefore expected to be positive. Indeed, the leading (one-loop) contribution – χ_1 – that refers to noninteracting spin waves, is positive and dominates the behavior of the system. However, the manifestation of the spin-wave interaction – or more general, Goldstone boson interaction – is more subtle, as we now discuss.

In order to measure the Goldstone boson interaction in the temperature-dependent part of the susceptibility, we define the dimensionless quantity

$$\xi_\chi(T, H_s) = \frac{\chi_{int}^{[2]}(T, H_s) + \chi_{int}^{[4]}(T, H_s)}{\chi_{Bose}(T, H_s)}. \quad (4.22)$$

In Fig. 9 we then plot the two-loop (T^2) and three-loop (T^4) contribution in $\xi_\chi(T, H_s)$ for three different temperatures ($T/F = 0.04, 0.07, 0.10$) and $N = \{2, 3, 4, 5, 6\}$. Note that we consider the behavior of the system in nonzero external field, i.e., away from the limit $H_s \rightarrow 0$ where the susceptibility diverges. Much like in the pressure and the order parameter, the spin-wave interaction in antiferromagnets only starts showing up at three-loop order.

The behavior of the $d=3+1$ quantum XY model is indeed peculiar, because the ratio $\xi_\chi(T, H_s)$ drops to negative values in weak external fields. This behavior persists at more elevated temperatures (see Fig. 9), and is contrary to all systems with $N \geq 4$ where $\xi_\chi(T, H_s)$ tends to large positive values in weak external fields. If the temperature is very low ($T/F = 0.04$), the parameter range where $\xi_\chi(T, H_s)$ is negative, is quite large for systems with $N \geq 4$. However, at more elevated temperatures, the quantity $\xi_\chi(T, H_s)$ may reach positive values, since three-loop corrections become large. In particular, in QCD where the NLO low-energy constants are known, $\xi_\chi(T, H_s)$ is positive in the entire parameter region M_π/F , as soon as the temperature exceeds $T/F \approx 0.20$. This is illustrated in Fig. 10. Also, in the physical region of QCD ($M_\pi \approx 139.6 MeV$), $\xi_\chi(T, H_s)$ is always positive and very weak at low temperatures: $\xi_\chi(T, H_s) \approx 10^{-6}$ for $T/F = 0.20$. We stress again that we are describing subtle two-loop and three-loop effects that manifest themselves in the temperature-

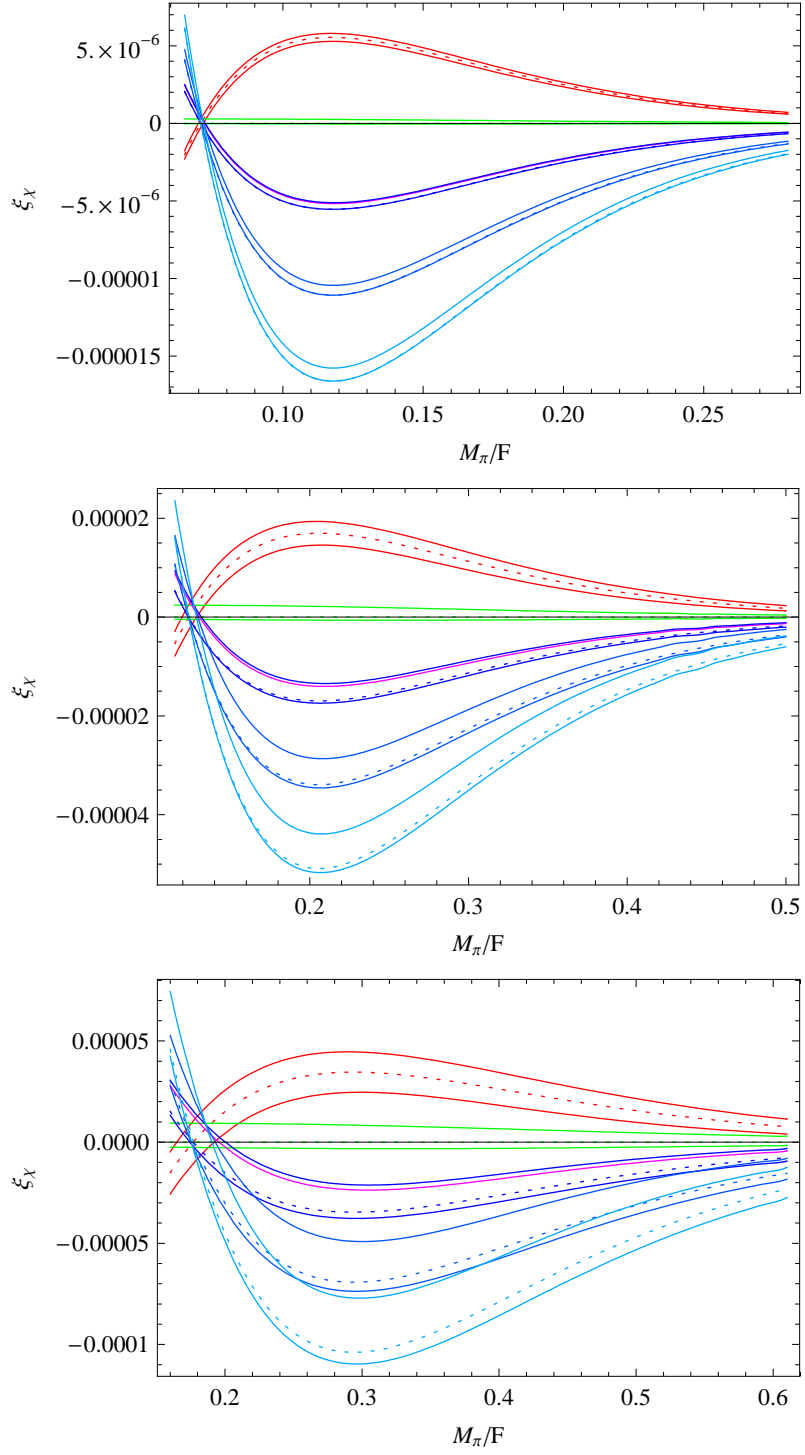


Figure 9: [Color online] Temperature-dependent Goldstone-boson interaction manifesting itself in the susceptibility of $d=(3+1)$ systems characterized by a spontaneously broken symmetry $O(N) \rightarrow O(N-1)$ for $N = \{2, 3, 4, 5, 6\}$ from top to bottom in the figure (vertical cut at $M_\pi/F = 0.25$): two-loop contribution (dashed curves) and sum of two-loop contribution and three-loop correction (continuous curves). The temperatures are $T/F = 0.04, 0.07, 0.10$ (top to bottom).

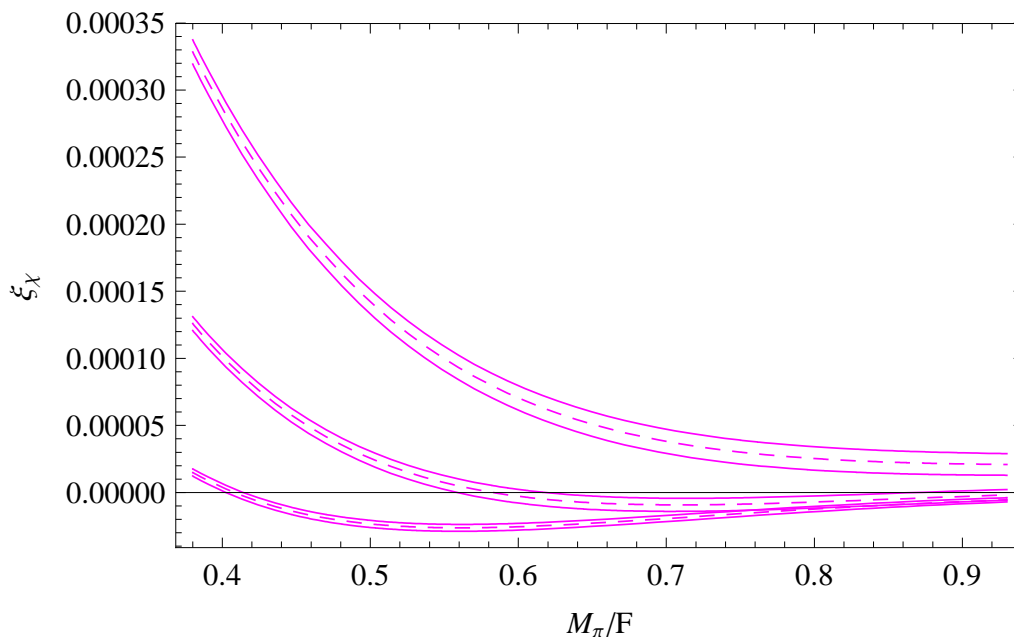


Figure 10: Quantum chromodynamics ($N=4$): Manifestation of the pion-pion interaction in the susceptibility. The curves refer to $T/F = \{0.17, 0.20, 0.23\}$ from bottom to top in the figure. The dashed curves correspond to the sum of the two- and three-loop correction. The error bars reflect the uncertainty in the values of the NLO effective constants $\bar{e}_1, \bar{e}_2, \bar{k}_1, \bar{k}_2$ – see Eqs. (4.8) and (4.9).

dependent interaction part of the susceptibility – these effects are weak compared to the dominant noninteracting (one-loop) contribution.

5 Conclusions

The low-temperature behavior of $d=3+1$ (pseudo-)Lorentz-invariant systems with a spontaneously broken internal symmetry $O(N) \rightarrow O(N-1)$ can be derived systematically and straightforwardly up to three loops using effective Lagrangians. Important physical realizations are the quantum XY model ($N=2$), the Heisenberg antiferromagnet ($N=3$), and two-flavor quantum chromodynamics ($N=4$).

From a conceptual point of view, the structure of the low-temperature series is of interest. In the nonabelian case, logarithmic contributions of the form $(T^2)^n \ln T$ emerge at the three-loop level, whereas in the abelian case we are dealing with simple powers of T^2 . The coefficients accompanying the terms in the low-temperature expansion, depend in a nontrivial way on the ratio H_s/T (where H_s is an external field), and furthermore involve low-energy effective constants that parametrize the microscopic details of the system.

One of our objectives was to investigate the impact of the Goldstone-boson interaction at finite temperature and nonzero external field onto the thermodynamics of the system. In the pressure, the dominant two-loop contribution may be repulsive ($N=2$), zero ($N=3$), or attractive ($N \geq 4$). Three-loop corrections – depending on sign and magnitude of the NLO low-energy constants $\bar{e}_1, \bar{e}_2, \bar{k}_1, \bar{k}_2$ – may go into either direction. Overall, the three-loop corrections become substantial at more elevated temperatures – as a result, the Goldstone boson interaction in the pressure may become repulsive irrespective of H_s .

While the dominant one-loop contribution in the order parameter (susceptibility) is negative (positive), the sum of the two- and three-loop correction may behave differently. These subtle effects, originating from the Goldstone boson interaction at finite temperature, are particularly pronounced at low temperatures where the two-loop contribution dominates over the three-loop correction. The $d=3+1$ quantum XY model is exceptional, since the temperature-dependent interaction contribution in the order parameter (susceptibility) tends to large positive (negative) values in weak external fields. These somehow counterintuitive effects do not occur in QCD at the physical pion mass.

The effective theory results regarding the Goldstone boson interaction, supersede well-cited results in the literature (e.g., Ref. [12]). Logarithmic terms in the low-temperature expansion of the order parameter of antiferromagnets have never been reported outside the effective Lagrangian framework. Regarding quantum XY models, the analysis at low temperatures where the spin waves dominate the physics of the system, has never been carried beyond one-loop order within the traditional microscopic perspective. In view of these shortcomings in the literature, one concludes that the systematic effective Lagrangian method is a very valuable tool to address the low-temperature properties of condensed matter systems.

As far as quantum chromodynamics is concerned, the subtle effects we observe in the pressure, quark condensate, and susceptibility, cannot be "seen" in present lattice simulations. Our figures refer to very low temperatures ($T \lesssim 0.2F$) and small (unphysical) pion masses. While this parameter region is currently not accessible on the lattice, it is our hope that the subtle effects reported here may be confirmed in future numerical studies.

It should be noted that our results are not restricted to quantum XY models, Heisenberg antiferromagnets, or two-flavor quantum chromodynamics – they also apply to other realizations of a specific N , provided the corresponding systems share the same symmetries. While the low-temperature series then present the same structure – powers of T^2 and logarithms $(T^2)^n \ln T$ – the difference concerns the specific numerical values of the effective constants that indeed depend on the system under consideration. This underlines the universal nature of the effective field theory approach. What counts are the symmetries of the system – the construction of the effective Lagrangian then becomes a straightforward group-theoretical exercise and

the corresponding effective field-theory predictions are universal.

Acknowledgments

The author thanks A. Gómez Nicola, H. Leutwyler, A. Smilga and U. Wenger for correspondence.

A Renormalization

In this appendix we discuss some technical issues regarding renormalization. We start with the Goldstone boson mass M_π that we have defined in Eq. (3.3),⁸

$$M_\pi^2 = \frac{\Sigma_s H_s}{F^2} + \left[2(k_2 - k_1) + (N - 3)\lambda \right] \frac{(\Sigma_s H_s)^2}{F^6} + c \frac{(\Sigma_s H_s)^3}{F^{10}} + \mathcal{O}(H_s^4), \quad (\text{A.1})$$

and the parameters a and b defined in Eq. (3.4),

$$\begin{aligned} a &= -\frac{(N-1)(N-3)}{32\pi} \frac{\Sigma_s H_s}{F^4} + \frac{N-1}{4\pi} \frac{(\Sigma_s H_s)^2}{F^8} \left\{ \left[(N+1)(e_1 + e_2) + k_2 - k_1 \right] \right. \\ &\quad \left. - \frac{(N-1)^2}{2} \lambda - \frac{3N^2 + 32N - 67}{768\pi^2} \right\}, \\ b &= \frac{N-1}{\pi F^4} \left\{ \left[2e_1 + Ne_2 \right] - \frac{5(N-2)}{3} \lambda - \frac{N-2}{16\pi^2} \right\}. \end{aligned} \quad (\text{A.2})$$

These expressions involve unrenormalized (infinite) NLO effective constants: e_1, e_2, k_1 and k_2 . Denoting these quantities as l_i ($i = 1, 2, 3, 4$), and adopting the standard convention of chiral perturbation theory (for details see, e.g., Ref. [45]),

$$l_i = \tilde{\gamma}_i \left(\lambda + \frac{1}{32\pi^2} \bar{l}_i \right), \quad (\text{A.3})$$

the singular expression λ – see Eq. (3.5) – in M_π, a and b can be eliminated,

$$M_\pi^2 = \frac{\Sigma_s H_s}{F^2} + \frac{\tilde{\gamma}_4 \bar{k}_2 - \tilde{\gamma}_3 \bar{k}_1}{16\pi^2} \frac{(\Sigma_s H_s)^2}{F^6} + \mathcal{O}(H_s^3), \quad (\text{A.4})$$

⁸The explicit expression for the constant c that involves next-to-next-to-leading order effective constants is not needed here.

$$\begin{aligned}
a &= -\frac{(N-1)(N-3)}{32\pi} \frac{\Sigma_s H_s}{F^4} + \frac{N-1}{128\pi^3} \frac{(\Sigma_s H_s)^2}{F^8} \\
&\quad \times \left\{ (N+1)(\tilde{\gamma}_1 \bar{e}_1 + \tilde{\gamma}_2 \bar{e}_2) + \tilde{\gamma}_4 \bar{k}_2 - \tilde{\gamma}_3 \bar{k}_1 - \frac{3N^2 + 32N - 67}{24} \right\}, \\
b &= \frac{N-1}{32\pi^3 F^4} \left\{ 2\tilde{\gamma}_1 \bar{e}_1 + N\tilde{\gamma}_2 \bar{e}_2 - 2(N-2) \right\}.
\end{aligned} \tag{A.5}$$

Up to a factor of $\tilde{\gamma}_i/32\pi^2$, the constants \bar{l}_i are the so-called running coupling constants at the fixed scale $\mu = \hat{M}_\pi$, where $\hat{M}_\pi \approx 139.6 \text{ MeV}$ is the physical pion mass. The quantities $\tilde{\gamma}_i$ are coefficients of order one. To avoid confusion, we explicitly provide our renormalization conventions:

$$\begin{aligned}
e_1 &= \tilde{\gamma}_1 \left(\lambda + \frac{1}{32\pi^2} \bar{e}_1 \right), & e_2 &= \tilde{\gamma}_2 \left(\lambda + \frac{1}{32\pi^2} \bar{e}_2 \right), & k_1 &= \tilde{\gamma}_3 \left(\lambda + \frac{1}{32\pi^2} \bar{k}_1 \right), \\
k_2 &= \tilde{\gamma}_4 \left(\lambda + \frac{1}{32\pi^2} \bar{k}_2 \right).
\end{aligned} \tag{A.6}$$

The fact that the singular quantity λ must drop out in the renormalized expressions M_π, a, b , implies various consistency conditions among the coefficients $\tilde{\gamma}_i$. From the renormalization of M_π^2 one concludes

$$\tilde{\gamma}_4 - \tilde{\gamma}_3 = -\frac{(N-3)}{2}. \tag{A.7}$$

Invoking the renormalization of the parameters a and b one obtains

$$\begin{aligned}
\tilde{\gamma}_1 &= \frac{3N-10}{6}, & \tilde{\gamma}_2 &= \frac{2}{3}, & (N \neq 2), \\
\tilde{\gamma}_1 + \tilde{\gamma}_2 &= 0, & (N = 2).
\end{aligned} \tag{A.8}$$

In QCD ($N=4$), according to Ref. [45], we have $\tilde{\gamma}_1 = \frac{1}{3}$, $\tilde{\gamma}_2 = \frac{2}{3}$, $\tilde{\gamma}_4 - \tilde{\gamma}_3 = -\frac{1}{2}$: indeed, the above consistency conditions are satisfied.

The renormalized NLO effective constants \bar{l}_i depend on the pion mass M_π as follows:

$$\bar{l}_i = -\ln \left(\frac{M_\pi}{\hat{M}_\pi} \right)^2 + \hat{l}_i. \tag{A.9}$$

Here the \hat{l}_i are pure numbers of order one. While the mass M_π varies according to the strength of the field H_s , note that the mass \hat{M}_π corresponds to the physical (fixed) pion mass $\hat{M}_\pi = 139.6 \text{ MeV}$. To have a general relation that is also valid for $N \neq 4$, we rewrite Eq. (A.9) in the form

$$\bar{l}_i = -\ln \left(\frac{M_\pi/F}{\hat{M}_\pi/F} \right)^2 + \hat{l}_i, \tag{A.10}$$

where the masses are now given in relation to the leading-order effective constant F . In analogy to QCD, for $N \neq 4$ we choose the ratio in question as

$$\frac{\hat{M}_\pi}{F} \equiv \frac{139.6 \text{ MeV}}{86.8 \text{ MeV}} \approx 1.61. \quad (\text{A.11})$$

In connection with magnetic systems, \hat{M}_π corresponds to a (fixed) external field according to Eq. (3.3). It should be pointed out that the quantities \bar{l}_i become singular in the chiral limit $M_\pi \rightarrow 0$ ($|\vec{H}_s| \rightarrow 0$). It so seems that taking this limit in the free energy density – and in all thermodynamic observables derived from there – is problematic.

The crucial point, however, is the following: in the free energy density, Eq. (3.1), apart from the parameter b that explodes in the chiral limit, the function j also becomes singular if $M_\pi \rightarrow 0$,⁹

$$j(\tau) = \frac{5(N-1)(N-2)}{48} \ln \tau + \hat{j}(\tau), \quad \tau = \frac{T}{M_\pi}. \quad (\text{A.12})$$

Using the previous formulas, the parameter b – in the *nonabelian* case – can be rewritten as

$$b = -\frac{5(N-1)(N-2)}{48\pi^3 F^4} \ln \frac{M_\pi}{\Lambda_b}, \quad (N \neq 2), \quad (\text{A.13})$$

where the scale Λ_b involves NLO effective constants,

$$\Lambda_b = \hat{M}_\pi \exp \left[\frac{6\tilde{\gamma}_1 \hat{e}_1 + 3N\tilde{\gamma}_2 \hat{e}_2}{10(N-2)} - \frac{3}{5} \right], \quad (N \neq 2). \quad (\text{A.14})$$

The coefficient of the logarithm in b is proportional to $(N-1)(N-2)$, much like the coefficient of the logarithm that appears in $j(\tau)$. Hence the two logarithms can be merged into a single logarithm that remains finite if $M_\pi \rightarrow 0$. More concretely, the relevant piece in the representation of the free energy density, Eq. (3.1), is

$$g \left[b - \frac{j}{\pi^3 F^4} \right] = h \left[b - \frac{j}{\pi^3 F^4} \right] T^8. \quad (\text{A.15})$$

Since the limit $M_\pi \rightarrow 0$ plays a special role, we decompose the functions h and j as

$$h(\tau) = \frac{\pi^4}{675} + \tilde{h}(\tau), \quad j(\tau) = \nu \ln \tau + j_1 + \tilde{j}(\tau), \quad \nu = \frac{5(N-1)(N-2)}{48}. \quad (\text{A.16})$$

For $M_\pi \rightarrow 0$ (and T fixed), the remainders $\tilde{h}(\tau)$ and $\tilde{j}(\tau)$ tend to zero by construction. Using the representations (A.13) and (A.16), we end up with three contributions,

$$\begin{aligned} h \left[b - \frac{j}{\pi^3 F^4} \right] &= \frac{1}{32\pi^2} \left\{ 2\tilde{\gamma}_1 \bar{e}_1 + N\tilde{\gamma}_2 \bar{e}_2 - 2(N-2) \right\} \tilde{h}(\sigma) \\ &\quad - \frac{1}{N-1} \left\{ \frac{\pi^2}{675} \tilde{j}(\sigma) + \frac{j(\sigma) \tilde{h}(\sigma)}{\pi^2} \right\} + \frac{(N-2)\pi^2}{6480} \ln \left(\frac{\Lambda_P}{T} \right). \end{aligned} \quad (\text{A.17})$$

⁹Note that the parameter a tends to zero in the chiral limit.

In the chiral limit, only the last term survives. The scale Λ_P is defined by

$$\begin{aligned}\Lambda_P &= \hat{M}_\pi \exp \left[\frac{6\tilde{\gamma}_1\hat{e}_1 + 3N\tilde{\gamma}_2\hat{e}_2}{10(N-2)} - \frac{3}{5} - \frac{48j_1}{5(N-1)(N-2)} \right], \quad (N \neq 2), \\ &= \Lambda_b \exp \left[-\frac{48j_1}{5(N-1)(N-2)} \right].\end{aligned}\tag{A.18}$$

We have evaluated the coefficients j_1 following the procedure described in Ref. [24]. The results are provided in the second column of Table 1 for $N = \{3, 4, 5, 6\}$.

N	ν	j_1	j_2
3	5/24	0.1122	0.0363
4	5/8	0.3366	0.119
5	5/4	0.6731	0.260
6	25/12	1.122	0.472

Table 1: *The coefficients ν , j_1 and j_2 referring to the three-loop function $j(\tau)$.*

Collecting results, the low-temperature expansion for the pressure $P = z_0 - z$ takes the form

$$\begin{aligned}P &= \frac{1}{2}(N-1)h_0T^4 - \frac{(N-1)(N-3)}{8F^2t^2}h_1^2T^6 \\ &+ \frac{N-1}{32\pi^2F^4\tau^4} \left\{ (N+1)(\tilde{\gamma}_1\bar{e}_1 + \tilde{\gamma}_2\bar{e}_2) + \tilde{\gamma}_4\bar{k}_2 - \tilde{\gamma}_3\bar{k}_1 - \frac{3N^2 + 32N - 67}{24} \right\} h_1^2T^8 \\ &+ \frac{(N-1)(N-2)\pi^2}{6480F^4}T^8 \ln\left(\frac{\Lambda_P}{T}\right) + \frac{N-1}{32\pi^2F^4} \left\{ 2\tilde{\gamma}_1\bar{e}_1 + N\tilde{\gamma}_2\bar{e}_2 - 2(N-2) \right\} \tilde{h}T^8 \\ &- \frac{1}{F^4} \left\{ \frac{\pi^2}{675}\tilde{j} + \frac{j\tilde{h}}{\pi^2} \right\} T^8.\end{aligned}\tag{A.19}$$

This representation is valid for the nonabelian case $N \geq 3$. In the abelian case, matters are much simpler because the singular piece λ in the parameter b , Eq. (A.2), does not occur. Here the combination $e_1 + e_2$ is finite – in particular, it does not explode in the chiral limit. Likewise, for $N=2$, the three-loop function j tends to zero in the chiral limit and does not become singular – everything is consistent also in the abelian case, where no logarithmic contribution $T^8 \ln T$ in the free energy density or pressure emerges.

In the low-temperature expansion of the order parameter, another scale – Λ_Σ – enters at order $T^6 \ln T$. It is related to the scale Λ_P showing up in the pressure by

$$\Lambda_\Sigma = \Lambda_P \exp \left(\frac{4\pi^2}{15\nu} j_2 \right).\tag{A.20}$$

The above coefficients j_2 occur in the expansion of the function $\tilde{j}(\tau)$,

$$\tilde{j}(\tau) = \frac{j_2}{\tau^2} + \frac{j_3}{\tau^3} + \mathcal{O}(\tau^{-4}),\tag{A.21}$$

and are listed in the third column of Table 1 for $N = \{3, 4, 5, 6\}$.

When evaluating the order parameter and the susceptibility on the basis of the representation for the pressure, Eq. (A.19), one should keep in mind that the renormalized NLO effective constants obey

$$\frac{\partial \bar{l}_i}{\partial M^2} = -\frac{1}{M^2}. \quad (\text{A.22})$$

Again, NLO effective constants that are not renormalized, do not depend on M (or $|\vec{H}_s|$).

References

- [1] C. P. Hofmann, J. Stat. Mech. **(2016)**, 093102.
- [2] D. D. Betts, C. J. Elliott and M. H. Lee, Can. J. Phys. **48**, 1566 (1970).
- [3] J. Oitmaa and D. D. Betts, Phys. Lett. A **68**, 450 (1978).
- [4] M. Uchinami, S. Takada and F. Takano, J. Phys. Soc. Jpn. **47**, 1047 (1979).
- [5] T. Aoki, S. Homma and H. Nakano, Prog. Theor. Phys. **64**, 448 (1980).
- [6] T. Aoki, S. Homma and H. Nakano, Prog. Theor. Phys. **66**, 861 (1981).
- [7] Z. Weihong, J. Oitmaa and C. J. Hamer, Phys. Rev. B **44**, 11869 (1991).
- [8] J. Oitmaa, C. J. Hamer and Z. Weihong, Phys. Rev. B **50**, 3877 (1994).
- [9] M. E. Gouvea and A. S. T. Pires, Phys. Rev. B **54**, 14907 (1996).
- [10] J. Schulenburg, J. S. Flynn, D. D. Betts and J. Richter, Eur. Phys. J. B **21**, 191 (2001).
- [11] A. Cucchieri, J. Engels, S. Holtmann, T. Mendes and T. Schulze, J. Phys. A: Math. Gen. **35**, 6517 (2002).
- [12] T. Oguchi, Phys. Rev. **117**, 117 (1960).
- [13] F. Keffer and R. Loudon, J. Appl. Phys. (Suppl.) **32**, 2 (1961).
- [14] T. Oguchi and A. Honma, J. Appl. Phys. **34**, 1153 (1963).
- [15] A. I. Akhiezer, V. G. Baryakhtar and M. I. Kaganov, Sov. Phys. Usp. **3**, 567 (1961).
- [16] A. I. Akhiezer, V. G. Baryakhtar and M. I. Kaganov, Sov. Phys. Usp. **4**, 661 (1961).

- [17] A. Brooks Harris, J. Appl. Phys. **35**, 798 (1964).
- [18] F. B. Anderson and H. B. Callen, Phys. Rev. **136**, A1068 (1964).
- [19] S. H. Liu, Phys. Rev. **142**, 267 (1966).
- [20] O. Nagai and T. Tanaka, Phys. Rev. **188**, 821 (1969).
- [21] M. G. Cottam and R. B. Stinchcombe, J. Phys. C: Solid St. Phys. **3**, 2326 (1970).
- [22] L. Flax and J. C. Raich, Phys. Rev. B **2**, 1338 (1970).
- [23] D. K. Ghosh, Phys. Rev. B **8**, 392 (1973).
- [24] P. Gerber and H. Leutwyler, Nucl. Phys. B **321**, 387 (1989).
- [25] A. Smilga and J. J. M. Verbaarschot, Phys. Rev. D **54**, 1087 (1996).
- [26] A. V. Smilga, Phys. Rept. **291**, 1 (1997).
- [27] S. Nam and C.-W. Kao, Phys. Rev. D **82**, 096001 (2010).
- [28] A. Gómez Nicola and R. Torres Andrés, Phys. Rev. D **83**, 076005 (2011).
- [29] R. Torres Andrés and A. Gómez Nicola, Prog. Part. Nucl. Phys. **67**, 337 (2012).
- [30] Y. Aoki et al., JHEP **0906**, 088 (2009).
- [31] A. Bazavov et al. (HotQCD Collaboration), Phys. Rev. D **85**, 054503 (2012).
- [32] A. Bazavov et al. (HotQCD Collaboration), Phys. Rev. D **86**, 034509 (2012).
- [33] M. I. Buchoff et al., Phys. Rev. D **89**, 054514 (2014).
- [34] T. Bhattacharya et al., Phys. Rev. Lett. **113**, 082001 (2014).
- [35] A. Bazavov et al. (HotQCD Collaboration), Phys. Rev. D **90**, 094503 (2014).
- [36] Sz. Borsanyi et al., arXiv:1510.03376.
- [37] H. Leutwyler, Phys. Rev. D **49**, 3033 (1994).
- [38] J. O. Andersen, T. Brauner, C. P. Hofmann, and A. Vuorinen, JHEP **1408**, 088 (2014).
- [39] C. P. Hofmann, Phys. Rev. B **60**, 406 (1999).
- [40] H. Leutwyler, in *Hadron Physics 94 – Topics on the Structure and Interaction of Hadronic Systems*, edited by V. E. Herscovitz, C. A. Z. Vasconcellos and E. Ferreira (World Scientific, Singapore, 1995), p. 1.
- [41] S. Scherer, Adv. Nucl. Phys. **27**, 277 (2003).

- [42] T. Brauner, *Symmetry* **2**, 609 (2010).
- [43] A. Manohar and H. Georgi, *Nucl. Phys. B* **234**, 189 (1984).
- [44] B. Gavela, E. E. Jenkins, A. V. Manohar and L. Merlo, arXiv:1601.07551.
- [45] J. Gasser and H. Leutwyler, *Ann. Phys.* **158**, 142 (1984).
- [46] C. Colangelo, J. Gasser, and H. Leutwyler, *Nucl. Phys. B* **603**, 125 (2001).
- [47] J. Bijnens and G. Ecker, *Ann. Rev. Nucl. Part. Sci.* **64**, 149 (2014).